

# Role of Edge Superconducting States in Trapping of Multi-Quanta Vortices by Microholes. Application of the Bitter Decoration Technique

A. Bezryadin and B. Pannetier

CRTBT-CNRS, B.P. 166, 38042, Grenoble, France

(Received April 28, 1995; revised August 11, 1995)

*The Bitter decoration technique is used to study the trapping of single and multiple quanta vortices by a lattice of circular microholes. By keeping a thin superconducting layer (the bottom) inside each hole we are able to visualise the trapped vortices. From this we determine, for the first time, the filling factor  $FF$ , i.e. the number of vortices captured inside a hole. In all cases the sample is cooled at a constant field before making the decoration. Two qualitatively different states of the vortex crystal are observed: (i) In case when the interhole distance is much larger than the coherence length, the filling factor averaged over many identical holes ( $\langle FF \rangle$ ) is a stepwise function of the magnetic flux (of the external field) through the hole, because each hole captures the same number of vortices. The density of fluxoids inside the openings is higher than in the uniform film, but much lower than it should be in the state of equilibrium. We claim that the number of trapped vortices is determined by the edge superconducting states which appear around each hole at the modified third critical field  $H_{c3}^* > H_{c2}$ . Below  $H_{c2}$  such states produce a surface barrier of a new type. This barrier for the vortex entrance and exit is due to the strong increase of the order parameter near the hole edge. It keeps constant the number of captured vortices during the cooling at a fixed field. (ii) An increase of the hole density or of the hole radius initiates a sharp redistribution of fluxoids: all of them drop inside holes. This first order transition leads to a localization of all vortices and consequently to a qualitative change of the transport properties (TAFF in our case). In the resulting new state the filling factor is not any more the same for neighbouring holes and its averaged value is equal to the frustration of the hole network.*

## 1. INTRODUCTION

While considering the vortex pinning by parallel (to vortices) dielectric cylindrical microchannels (columnar defects for example) or by microholes

in a thin film, one can distinguish two qualitatively different limiting cases: (1) The London limit (LL) takes place when the external magnetic field ( $H$ ) is much smaller than the second critical field  $H_{c2}(T)$  ( $T$  is the temperature). In this case the order parameter modulation is negligible and vortices can be introduced as  $\delta$ -functions in the right part of the London equation. The vortex distribution and the pinning can be found from the London free energy which includes the kinetic energy of supercurrents and the energy of essentially non-uniform magnetic field. In the LL one should assure that the channel radius is much larger than the temperature dependent coherence length ( $\xi = \xi(T)$ ). (2) The opposite case when  $H \approx H_{c2}(T)$  can be referred as the Ginzburg-Landau limit (GLL). In this case the spatial modulation of the order parameter is crucial and one should use the Ginzburg-Landau (GL) free energy to analyse the vortex distribution and the pinning by empty channels (or by microholes). At the same time the magnetic field modulation inside the sample can be neglected in this limit. Note that in both cases we assume that the Ginzburg-Landau parameter  $\kappa = \lambda/\xi \gg 1$  (here and below  $\lambda = \lambda(T)$  is the magnetic screening length). In the GLL the coherence length is of the order of the channel radius ( $R$ ) if  $\pi R^2 H \approx \phi_0$  (where  $\phi_0 = 2.07 \cdot 10^{-7}$  Oe  $\cdot$  cm<sup>2</sup> is the flux quantum). Also, it is remarkable that the problem of the vortex distribution in the Ginzburg-Landau limit is similar to the quantum mechanical problem of a *single* charged particle confined inside the volume of the sample under consideration and exposed to the same magnetic field. Indeed, at the critical field the vortex positions are given by zeros of the single particle wave function of the ground state; the critical temperature is determined by the energy of the ground state.

The vortex pinning in pierced superconductors and the problem of the multi-quanta vortices has been analysed in many theoretical<sup>1, 2, 3, 4</sup> and experimental<sup>5, 6</sup> papers, but usually in the London Limit. The Ginzburg-Landau limit is not so well developed. It was considered for the first time theoretically by Ovchinnikov.<sup>7</sup>

In our present work we analyse experimentally the vortex distribution in a film with a lattice of circular holes in the GLL. It should be emphasized that our experiment is an indirect one because the Bitter decoration can be done only at low temperature when the applied field is already much smaller than  $H_{c2}(T)$ . Nevertheless we will argue that the freezing effect should take place, in other words the vortex distribution once determined at the nucleation temperature is not changed significantly during the field cooling. In this sense the obtained results are relevant to the properties of the system at  $H_{c2}(T) \approx H$  (GLL) when the coherence length is comparable to the radius of the holes.

It is well known that near the surface of a superconductor a non zero order parameter persists till the third critical field  $H_{c3}(T) = 1.695 H_{c2}(T)$ . It

is the usual effect of surface superconductivity<sup>8</sup> which can be observed if the applied field is parallel to the sample surface. Similar effects were predicted for an infinite superconductor with an empty cylindrical channel (of arbitrary radius) if the field is parallel to the channel.<sup>9, 3</sup> In such case the critical field near the cavity (modified third critical field  $H_{c3}^* \equiv H_{c3}^*(T)$ ) is still higher than  $H_{c2}$  but lower than  $H_{c3}$ . Due to the fact that the sample is multiply connected, the critical field is an oscillating function of the radius similarly to the Little-Parks effect.<sup>8</sup> In our previous work<sup>10</sup> it was shown experimentally that the enhancement of the critical field takes place also in a thin film near the edge of a microhole when the field is perpendicular to the film plane. In fact these two configurations: a thin superconducting film with a hole in perpendicular magnetic field and a 3-D superconductor with a cylindrical empty channel in coaxial field are equivalent in the GLL (if the thermal fluctuations are negligible). As in the usual effect of surface superconductivity,<sup>11, 12</sup> a region of strongly enhanced order parameter exists near the hole edge both above and slightly below  $H_{c2}$  (just because the critical field is higher near the edge). Of course this maximum is essential only near  $H_{c2}$  (more precisely, when  $H_{c2} - H \ll H_{c3}^* - H_{c2}$ , or when  $H > H_{c2}$ ), while at lower fields (in the LL) the order parameter is almost uniform in the sample. In fact the important difference between GLL and LL is that in the GLL the interaction of vortices with holes (repulsion if  $FF > 0$ ) strongly dominates the interaction between vortices themselves because of the strong maximum of the order parameter around holes (it can be much higher than the averaged order parameter far from the hole). This maximum creates a new type of surface barrier ( $\psi$ -barrier) for the vortex entrance and exit which helps (together with the intrinsic pinning in the film) to conserve down to  $T=0$  K approximately the same number of vortices inside each hole as have been nucleated at  $T_{c3}^*$ . The last statement is a hypothesis which we will verify experimentally. Note that  $T_{c3}^* \equiv T_{c3}^*(H)$  and  $T_{c2} \equiv T_{c2}(H)$  are temperatures when the applied field is equal to  $H_{c3}^*(T)$  and  $H_{c2}(T)$ , respectively. An important difference of the introduced above  $\psi$ -barrier (which exists only in GLL) and the well known Bean-Livingston barrier is the scale on which the barrier is localised. The Bean-Livingston barrier is due to the competition of the image force and the Lorentz force caused by the current circulating around a hole if at least one vortex is captured already. Its thickness is of the order of  $\lambda(T)$  (in thin films  $\lambda(T)$  should be replaced by  $\lambda^2/d_f$  where  $d_f$  is the film thickness). In contrast, the thickness of the  $\psi$ -barrier is about  $\xi(T)$ . In amorphous films or in HTSC it can be a very small value (20 Å for example), much smaller than  $\lambda(T)$ . Such difference of this two barriers should be important for the quantum tunnelling of vortices in the holes which depends exponentially on the barrier thickness as well as on its height.

Here we use the Bitter decoration technique (Section 2) to visualize individual vortices in a perforated superconducting Nb film after a cooling at a constant perpendicular magnetic field. A not fully completed perforation is used to create so called “blind” holes. This approach made possible the Bitter decoration of vortices trapped by the microholes. The results are presented in Section 3. Mostly we are interested in the number of vortices which can be captured by a hole of a given radius during the field cooling (this number will be named “filling factor”,  $FF$ ). Two qualitatively different regimes are analysed: the limit of independent (Section 4) and strongly interacting (Section 5) holes. Earlier the capturing of multiple quanta vortices was considered theoretically from the energetic point of view but we will show that a strongly non equilibrium vortex distribution is realised after the field cooling. The previous experimental results<sup>5, 6</sup> are concerned only with averaged properties of the ensemble of vortices in a sample with a lattice of holes while here a microscopic approach is developed.

The last part of the paper is devoted to collective effects. We discuss (in the Section 5) the origin of the transition in the film with a lattice of holes observed in our previous work.<sup>10</sup> It was found that the critical temperature  $T_{c3}^*(H)$  of the perforated film is an oscillating function of the field. When the field is high enough, the critical temperature exhibits so-called “single-object” oscillation with a relatively large period determined by the hole area and with down-directed cusps as in the Little-Parks experiment. At low fields, a so-called “collective” oscillation is found with a small period determined by the distance between the holes and up-directed cusps as it is usual for the critical temperature of superconducting wire networks.<sup>13</sup> The transition between these two types of behaviour takes place at such field when the coherence length at the critical temperature  $T_{c3}^*(H)$  is approximately equal to the interhole distance. From the general point of view, each cusp of the “collective” oscillation in  $T_{c3}^*(H)$  corresponds to the formation of a periodic superlattice of vortices commensurate with the lattice of holes. An important question arises whether the vortices of the superlattice sit inside holes or in the interstices. The Bitter decoration shows that all vortices are in the holes. A brief analysis of transport properties just below the transition (in the GLL) is also presented in the Section 5.

## 2. EXPERIMENTAL TECHNIQUE

The principle of the Bitter decoration which is used here to visualise vortices in the superconducting film consists in the evaporation of a small amount of a ferromagnetic metal (60  $\mu\text{g}$  of Ni in our case) near the sample surface. The resulting smoke of small ferromagnetic particles (their

size is of the order of  $100 \text{ \AA}$ ) is attracted by the magnetic field gradient which is due to the vortex currents. Finally the positions where the vortices cross the sample surface are marked by the particles and are visible in the electron microscope as white spots after the sample is heated to the room temperature.

All magnetic decorations<sup>14</sup> are done at  $T_{dec} \approx 4.2 \text{ K}$  and at a pressure of 0.6 mbar of the thermal exchange gas He after cooling at a fixed field of the order of 10 Oe. A thin Nb film ( $T_{c0} = 9.2 \text{ K}$ ) of a thickness  $d_f = 0.17 \text{ }\mu\text{m}$  with a triangular lattice of circular holes is used as a sample. The holes are organised in arrays. Each array contains about 50 identical holes which are forming a regular triangular lattice. The difference between the arrays is the hole radius or the lattice constant. The Nb epitaxial film is produced by electron beam evaporation of pure Nb at high vacuum (base pressure  $10^{-10}$  mbar) on a sapphire monocrystalline substrate maintained at  $550^\circ \text{ C}$ . The holes are made by the reactive ion etching (RIE) with the gas  $\text{SF}_6$ . Before the RIE, the film was covered with an electron sensitive resist (PMMA) and patterned by the  $e$ -beam lithography. The lattice parameter (the distance between the hole centers) is  $a = 3.2, 6.1, \text{ or } 12 \text{ }\mu\text{m}$ , the hole radius is swept from  $R = 0.15$  to  $R = 2.2 \text{ }\mu\text{m}$ .

A serious problem in the magnetic decoration of artificial microsystems, for example superconducting wire networks,<sup>14</sup> is the extremely weak magnetic field modulation. Really the amplitude of the field modulation (which determines the contrast of the resulting images) above a hole with one vortex is about  $\Delta H = \phi_0/R^2$  while for a vortex in a uniform film it is  $\Delta H = \phi_0/\lambda^2$ . In our experiments  $R \gg \lambda$  so the direct decoration of holes is ineffective. To eliminate such difficulty we put our system on a thin superconducting layer ("compression" layer) which changes very weakly the vortex distribution<sup>15</sup> but helps to visualise and count vortices captured inside holes. This method can be named "flux compression" because the large coreless vortices with a weak magnetic contrast captured inside relatively large holes are transformed inside the "compression" layer into compact Abrikosov vortices with a strong magnetic contrast which are routinely observed by the magnetic decoration. Technically the sample is prepared by decreasing the time of RIE. After the incomplete etching we obtain holes with a bottom (blind holes) which plays the role of the "compression" layer. Note that in such case this layer is a part of the system and naturally in a good electrical contact with the perforated film.

An important point in the usage of the "flux compression" method is to ensure that the displacement of vortices in the "compression" layer with respect to vortex positions in the sample is small with respect to the inter-vortex distance (such displacement can take place due to the intrinsic pinning in the "compression" layer). The smallness of the displacement is

achieved by making this layer to be very thin and in a perfect electrical contact with the sample. The last circumstance is important because if there is an insulating film between the system under investigation and the “compression layer” (even a very thin film) then a relative displacement of vortices in the sample and in the layer leads to the creation of a Josephson vortex parallel to the “compression” layer. The increase of the total energy is very weak in such case so the displacement can be large. In our geometry we can definitely distinguish between trapped vortices and vortices outside holes.

On the other hand the “compression” layer should not be thick because it can, in principle, change the vortex distribution in the sample. It was found that the Nb film thickness as small as 200 Å is already enough to visualise vortices by the decoration. In our experiments we use holes with a bottom of thickness  $d_b = 650$  Å (36 sec. of RIE). Some experiments are done with open holes (through holes without any bottom). In such case the captured vortices are not visible and one can determine the filling factor only by counting the rest of vortices outside holes (see below).

### 3. EXPERIMENTAL RESULTS

Micrographs of two parts of the sample: with and without holes are shown in Figs. 1b and 1a respectively. The average density of vortices is much smaller in the perforated part because some of them are captured by holes and invisible. Close to each hole there is a region which is almost free of vortices. The vortex lattice is disordered due to the intrinsic pinning in the Nb film. When all vortices in the micrograph are well defined, it is possible to determine the averaged (over many identical holes) filling factor  $\langle FF \rangle$  by counting the total number of vortices in two pictures with and without holes (Figs. 1b and 1a) having the same size and magnification and by division of the difference by the number of holes. Mathematically it can be expressed by a simple formula

$$\langle FF \rangle = \frac{\rho_{vu} - \rho_{vp}}{\rho_h} \quad (1)$$

where  $\rho_{vu}$  is the vortex density in the uniform film without holes (in fact  $\rho_{vu} = H/\phi_0$ ),  $\rho_{vp}$  is the density of vortices in the perforated part of the sample (here only vortices outside holes which are visible as white spots in Fig. 1b should be counted), and  $\rho_h$  is the density of holes. Such method can be successfully applied only when the density of holes is not much smaller than the density of vortices. In the opposite case a small error in the counted vortex number causes a large error in the filling factor.

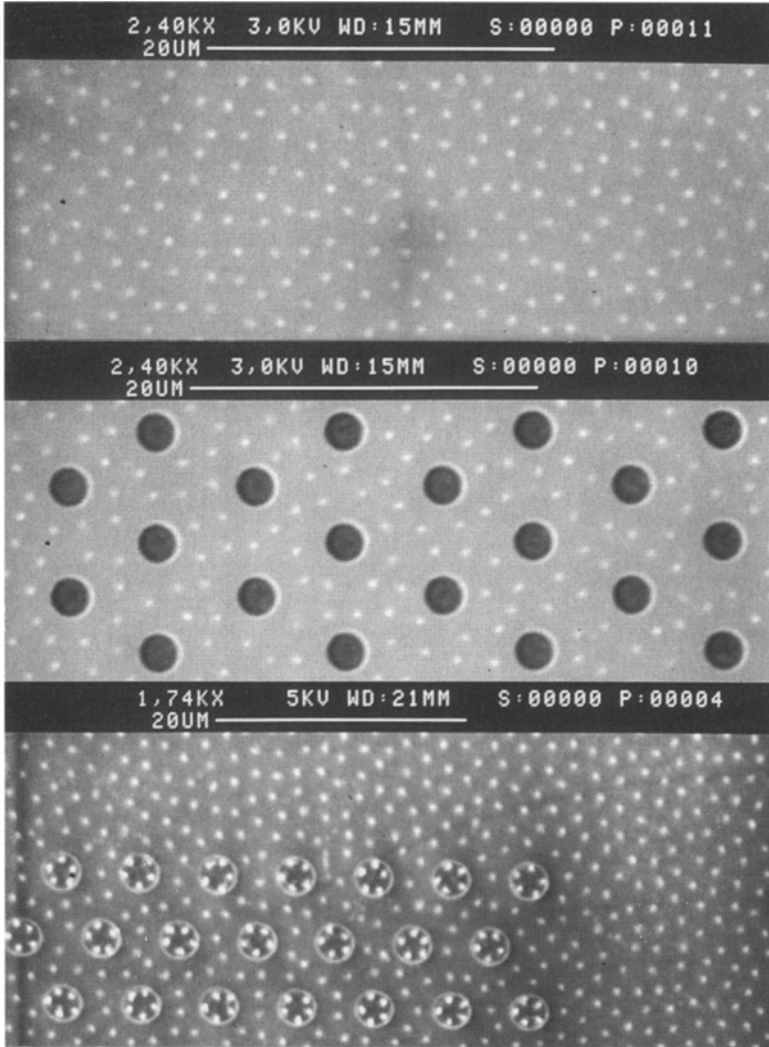


Fig. 1. Images of vortices (white spots) obtained with SEM after the magnetic decoration at 4.2 K in the perpendicular field  $H=6.37$  Oe (Figs. a, b, and c from the top to the bottom correspondingly). a: uniform Nb film of thickness  $0.17 \mu\text{m}$ ; b: the same film with a lattice of open holes of radius  $R=1.1 \mu\text{m}$ . Both pictures are obtained at the same conditions; c: Nb film of the same type with blind holes (bottom thickness  $d_b=0.65 \mu\text{m}$ ), each hole capture five vortices,  $R=1.49 \mu\text{m}$ .

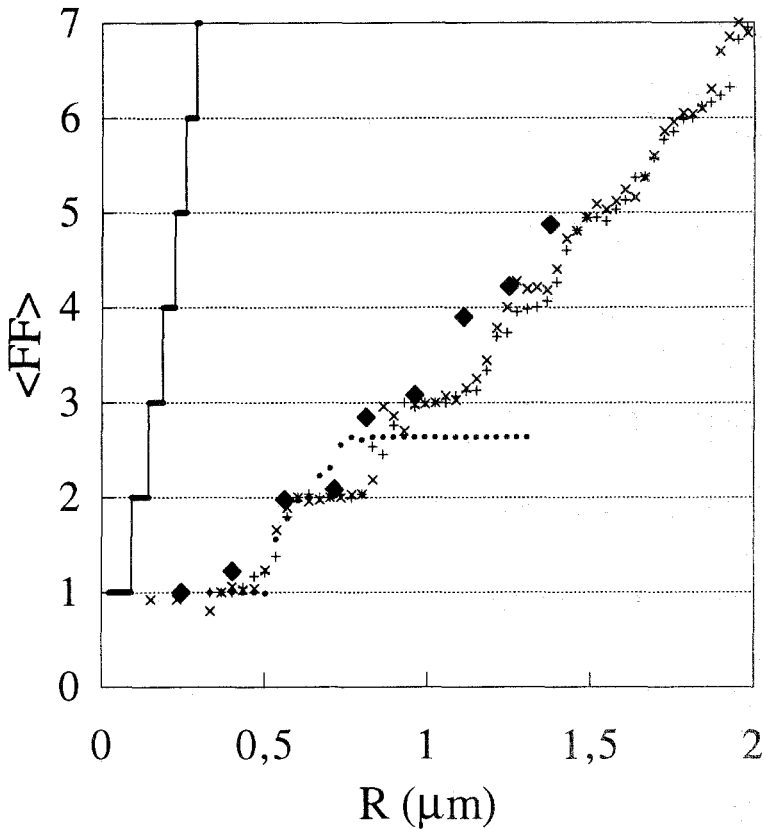


Fig. 2. Averaged (over about 50 identical holes) number of trapped vortices versus the hole radius,  $T = 4.2$  K,  $H = 6.37$  Oe; “♦”-open holes,  $a = 6.1 \mu\text{m}$ ; “x”-blind holes,  $d_b = 0.065 \mu\text{m}$ ,  $a = 6.11 \mu\text{m}$ ; “+”- $d_b = 0.65 \mu\text{m}$ ,  $a = 12 \mu\text{m}$ ; “•”- $d_b = 0.65 \mu\text{m}$ ,  $a = 3.2 \mu\text{m}$ ; the solid stepwise curve denotes the equilibrium filling factor at zero temperature.

The  $\langle FF \rangle$  value is determined by using the expression (1) in a number of hole arrays with the same  $a = 6.1 \mu\text{m}$  but with different  $R$  varied in the interval  $0.25 \mu\text{m} < R < 1.4 \mu\text{m}$ . The experimental points (Fig. 2, solid rhombuses) are concentrated near integer numbers.

As it is shown in Fig. 1c, captured vortices can be observed directly if each hole has a thin superconducting bottom (“flux compression” method). We find that each hole capture the same number of vortices (five in the picture) while the vortex lattice is disordered outside the holes. Inside holes vortices are arranged quite regularly (one can say to maximise the inter-vortex distance) and “attracted” to the hole edge. If  $FF$  is larger than 7 (for sufficiently large holes) then one vortex can be at the hole center (not



shown) while others are always near the edge. Note that the bottom thickness is uniform with an accuracy of 3%.

The decoration of blind holes shows that the bottom of a thickness about  $d_b = 0.065 \mu\text{m}$  changes very weakly the filling factor (the shift is about 10%). This is clear from Fig. 2 where we plot the averaged (over about 50 holes) value of the filling factor versus the hole radius for open (rhombuses) and blind (crosses) holes. This fact is in an agreement with the theoretical consideration<sup>15</sup> (see also the discussion below). Also one should take into account the possibility that the critical temperature of the bottom is slightly lower with respect to the film (due to the RIE process

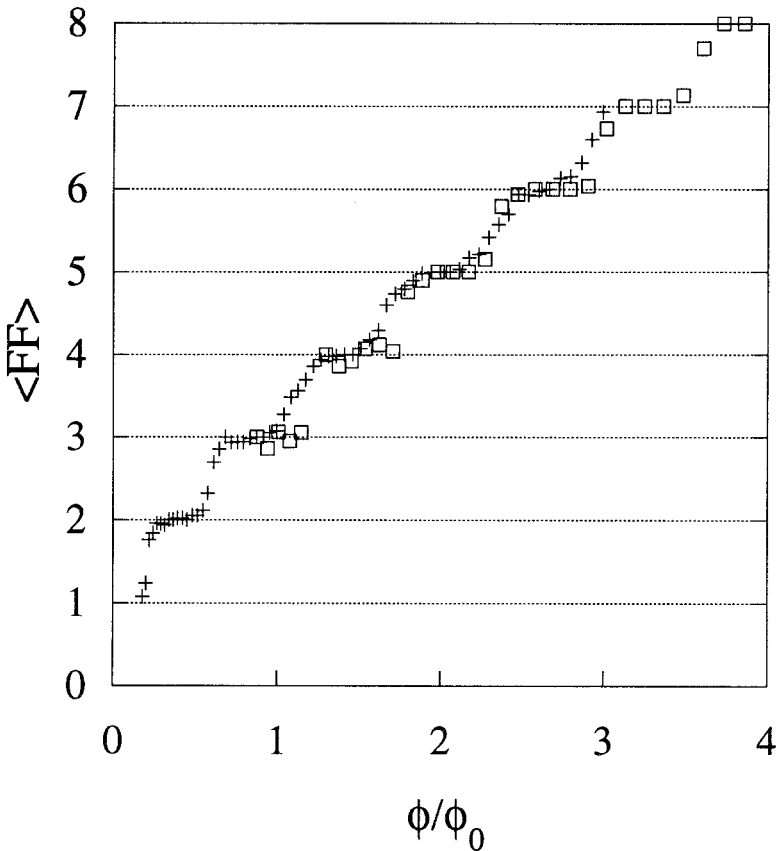


Fig. 3. Averaged (over about 50 identical holes) filling factor versus the reduced magnetic flux in the hole. The decorations are carried out after the sample has been cooled down to  $T = 4.2 \text{ K}$  at a constant field:  $H = 3.66 \text{ Oe}$  (crosses) or  $H = 9.55 \text{ Oe}$  (squares). Each experimental point corresponds to a new sample with some definite radius of holes.

and the small layer thickness). In such case the influence of the bottom on the filling factor should be even weaker.

A very good correlation between two curves corresponding to  $a = 6.1 \mu\text{m}$  and  $a = 12 \mu\text{m}$  (different types of crosses in Fig. 2) shows that the holes are practically independent because the increase of the lattice parameter by a factor of two does not change the filling factor. On the contrary in the case of the smallest period of the hole lattice  $a = 3.2 \mu\text{m}$  (solid dots) there is a strong collective effect which is discussed in the Section 5.

An interesting fact (Figs. 1c, 2, and 3) is the quantization of the averaged (over many holes) filling factor. Really in some definite ranges of  $R$  all the holes capture the same number of vortices while being surrounded by disordered external vortices. The  $\langle FF \rangle$  value is very close in such case to an integer number (see stepwise curves in Figs. 2 and 3). These special ranges of  $R$  are field dependent and in fact there is only one parameter which determines the  $\langle FF \rangle$ . This is the reduced flux of the external magnetic field through the hole area  $\phi/\phi_0 = \pi R^2 H/\phi_0$  ( $\phi_0$  is the flux quantum). The last statement is clear from Fig. 3 where we present two curves obtained at different fields:  $H = 3.66$  and  $9.55$  Oe (note that to sweep the flux we change the hole radius but not the field or, in other words, each experimental point corresponds to a new sample with a particular radius of holes). The curves practically coincide so one can conclude that only the flux determines the filling factor.<sup>16</sup>

For comparison with the theory it is useful to determine also the minimum value of the filling factor ( $FF_{\min}$ ), i.e. the minimum number of trapped vortices found among 50 identical holes of each array. This value (which is integer by definition) is equal to the  $\langle FF \rangle$  when  $\langle FF \rangle$  is integer because in such case all holes capture the same number of vortices. In all other experimental cases  $0 < \langle FF \rangle - FF_{\min} < 1$ . The experimentally found values of  $FF_{\min}$  (for  $H = 6.37$  Oe) are shown in Fig. 4a by solid circles.

#### 4. FILLING FACTOR OF AN INDEPENDENT HOLE

In this section we consider the case of a large separation between holes (much larger than the coherence length) when they are independent. The coincidence of the  $\langle FF \rangle$  for arrays with  $a = 6.1 \mu\text{m}$  and  $a = 12 \mu\text{m}$  (different crosses in Fig. 2) shows that such regime is achieved when  $a > 6 \mu\text{m}$  (and  $R < 2 \mu\text{m}$ ). The effects due to the interaction between holes are discussed in Section 5.

##### 4.1. Comparison with London Limit at Low Temperature

Let us compare firstly the experimental value of the  $\langle FF \rangle$  with the equilibrium (at the moment of decoration) filling factor which corresponds

to the minimum of the energy of the system. At low temperature when the decoration is done the system is in the London Limit because  $T_{dec} \approx 4.2 \text{ K} \ll T_{c3}^*(H)$  at any value of  $H$  used in our experiments. The distance between the vortices ( $a_v$ ) is much larger than the screening length ( $a_v \propto 1 \mu\text{m}$ ; the screening length in our Nb films<sup>17</sup> is  $\lambda(4.2 \text{ K}) \approx \lambda(0) \approx 1000 \text{ \AA}$ ) so the interaction between vortices is negligible. The thickness of the film ( $d_f = 1700 \text{ \AA}$ ) is larger than  $\lambda(0)$  so the result for an empty cylindrical channel in a 3-D infinite sample will be a good approximation. At last the size of holes ( $R \geq 1500 \text{ \AA}$ ) is much larger than the coherence length<sup>17</sup> ( $\xi(4.2 \text{ K}) \approx \xi(0) \approx 200 \text{ \AA}$ ) so the energy of vortices captured inside a hole can be found by using the London equation. The case of the equilibrium vortex distribution under the above conditions (in the LL) is considered in.<sup>3</sup> It is shown there that the trapping (by a hole) of a second vortex reduces the free energy of the system “hole with one trapped vortex” + “independent Abrikosov vortex at infinity” only if  $R > R_c(2) = \sqrt[3]{\lambda \xi^2}$  (note that the introduced here critical radius for the double quanta vortex nucleation  $R_c(2)$  is independent on the magnetic field if  $a_v \gg \lambda$ ). In our case the hole radius is always much larger than  $R_c(2) \approx 0.06 \mu\text{m}$ , so in the equilibrium state the filling factor should be  $\langle FF \rangle \geq 2$  in all cases. Experimentally we find  $\langle FF \rangle = 1$  till  $R > 0.5 \mu\text{m} \gg R_c$  (see Fig. 2).

With the same assumptions one can easily find (using the approach of ref. 1) the critical radius  $R_c(FF)$  for transitions  $FF-1 \rightarrow FF$  (entrance of one vortex into a hole with  $FF-1$  vortices inside). This critical radius follows from the condition that the free energy of a channel where  $FF$  vortices are trapped is equal to the energy of the same channel with  $FF-1$  vortices captured plus the energy of a free vortex at infinity. It is given by the following equation:

$$F_1 \left[ \frac{R_c(FF)}{\lambda} \right] = \frac{F_0}{2FF-1} \quad (2)$$

where  $F_0 = (H_c^2/4\pi)(2\pi/\kappa^2)(0.1 + \ln \kappa)$  is the energy of a free vortex at infinity,  $H_c$  is the thermodynamic critical field,  $\kappa = \lambda/\xi$  is the Ginzburg-Landau parameter,

$$F_1(R/\lambda) = \frac{H_c^2}{4\pi} \frac{\pi}{\kappa^2} \frac{K_0^2(R/\lambda)}{(K_1(R/\lambda) + RK_0(R/\lambda)/2)^2} \left[ 1 + \frac{2}{R/\lambda} \frac{K_1(R/\lambda)}{K_0(R/\lambda)} \right]$$

is the energy of single vortex trapped in a cylindrical channel of radius  $R$ , and  $K_0$  and  $K_1$  are modified Bessel functions. The result of the numerical calculation of the equilibrium (at zero temperature) filling factor is shown in Fig. 2 by the stepwise solid line (we accept  $\lambda(0) = 1000 \text{ \AA}$ ). Evidently the

filling of holes found in the experiment is far from the equilibrium. In such case one should consider higher temperatures, in other words the sample history, to explain the experimental data.

## 4.2. Edge States and Sample History

If a constant field is applied perpendicularly to the film and the temperature is decreased then a non-zero order parameter will appear for the first time at  $T = T_{c3}^*(H)$  near the hole edge in a thin belt of thickness  $\xi(T)$ . The order parameter  $\psi(\rho, \theta)$  decreases exponentially inside the superconductor:

$$\psi \propto e^{in\theta} \exp\left(-\frac{\rho^2}{\xi^2} \frac{H}{4H_{c2}}\right) \quad (3)$$

where  $(\rho, \theta)$  are the polar coordinates. One can define the number of vortices trapped by a hole at the superconductivity nucleation temperature as the increase in the phase of the order parameter (divided by  $2\pi$ ) after one turn around the hole:  $FF = n$ . The orbital number  $n$  in the formula (3) should be chosen to maximise  $T_{c3}^*$ . In principle to find the value of  $\langle FF \rangle$  at  $T = 0$  one should determine the probability of the vortex entrance (or exit) at all intermediate temperatures.

### 4.2.1. Region Below the $T_{c2}$

Let us consider the region below  $T_{c2}(H)$  when all the film is superconducting. In such case any increase of the filling factor corresponds with necessity to an approach and entrance of an Abrikosov vortex. If such motion of the vortex is not possible near the hole then the  $FF$  will be constant. Actually it is the case as we will see below.

Firstly, one can argue that the strong maximum of the amplitude  $|\psi|$  takes place near the hole edge not only above  $T_{c2}$  but also slightly below.<sup>12</sup> Numerical calculations<sup>18</sup> show that the order parameter amplitude near the hole edge at  $H = H_{c2}$  is very strong:  $|\psi|_{\rho=R, H=H_{c2}} \approx 0.5 |\psi|_{H=0}$ . At the same time at  $T_{c2}$  the superconductivity appears everywhere in the film as the Abrikosov vortex lattice but the amplitude of the averaged order parameter (and therefore the repulsion force between the vortices) is small in comparison to the  $|\psi|_{\rho=R}$  and proportional to the  $\sqrt{T_{c2} - T}$  (note that the  $|\psi|_{\rho=R}$  is proportional naturally to the  $\sqrt{T_{c3}^* - T}$  so it is finite even at  $T = T_{c2}$ ). The increase of  $|\psi|$  (when  $\rho \rightarrow R$ ) gives rise to a strong surface barrier because it leads to an increase of the condensation energy in the vortex core if the vortex approaches the hole, and therefore to a repulsion force acting on the vortex near the hole. It is evident that in such case

(more exactly when  $T_{c2} - T \ll T_{c3}^* - T_{c2}$  or  $H_{c2} - H \ll H_{c3}^* - H_{c2}$ ) the interaction between vortices is negligible with respect to the interaction between a vortex and the edge superconducting state. Note that due to the repulsion between vortices and the edge state we find a region free of vortices around each hole (Figs. 1b and 1c). It is conserved down to 4.2 K due to the intrinsic pinning.

Secondly, at temperatures considerably lower than  $T_{c2}(H)$  (in the LL) when the described above barrier is not efficient, the intrinsic pinning in the film is very strong, what is clear from the strongly disordered distribution of vortices in Fig. 1a. It implies that the filling factor should be constant also at low temperatures because vortices are pinned so they can not approach and enter the holes.

At last, another factor which helps to keep  $FF$  constant (at all temperatures) is the Bean-Livingston barrier. It is due to the supercurrent circulating around the hole if at least one vortex is already captured.<sup>1</sup> In this context one can remind that at the decoration temperature the condition  $a_v \gg \lambda$  is fulfilled, so the repulsion between vortices is negligible. Finally we come to the conclusion that the filling factor of an isolated hole should be constant during the field cooling from  $T_{c2}(H)$  down to zero temperature.

#### 4.2.2. Region Above $T_{c2}$

To analyse possibilities of transitions between different  $n$  above  $T_{c2}$  let us consider the phase diagram<sup>18</sup> of a film with a single hole in perpendicular field (Fig. 4b). The superconductivity nucleation near the hole is shown by the thin solid line (or by the dotted line for a blind hole with  $d_b/d_f = 0.382$ ). Temperatures when the free energies of states with orbital numbers  $n$  and  $n + 1$  are equal to each other, are shown by dashed lines (in the diagram the temperature is replaced for convenience by the temperature dependent coherence length  $\xi(T) = \xi(0)(1 - (T/T_{c0}))^{-1/2}$  normalised to the magnetic length given by the relation  $\pi L_H^2 = \phi_0$ ). The boundaries between states with different  $n$  are not parallel to the temperature axis so even if the field is fixed, the cooling can cause a first order phase transition with an increase of the filling factor by one. Note that no more than one such transition is possible in the interval  $T_{c2} < T < T_{c3}^*$ . It is clear that even if all possible (above  $T_{c2}$ ) first order transitions are realised, the curve  $FF(\phi/\phi_0)$  will have only a small shift to the left (about 10%) which is inversely proportional to the slope of the dashed lines in Fig. 4b. The shift can be larger if the screening effects are considerable (the first order transition boundaries shown in Fig. 4b are found in the limit of zero film thickness when the magnetic field is uniform inside the sample). Also a supercooling process is possible.

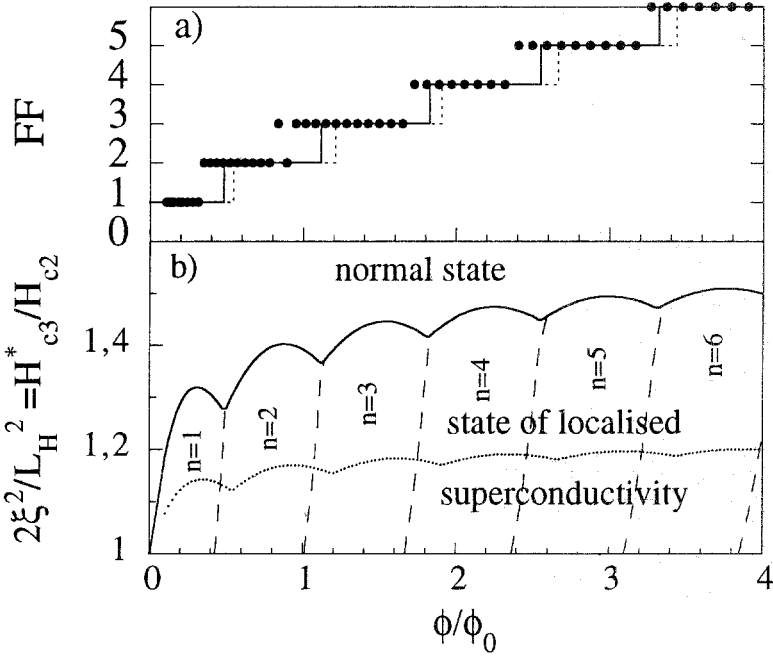


Fig. 4. (a) The solid circles denote the minimum value of the filling factor (found experimentally among 50 holes for the case  $a = 12 \mu\text{m}$ ,  $H = 6.37 \text{ Oe}$ ,  $d_b/d_f = 0.382$ ) versus the flux. The calculated number of vortices which nucleate inside each hole at  $T_{c3}^*$  is shown by the solid line for open holes and by the dashed line for blind holes with  $d_b/d_f = 0.382$ . Note that the moments when the theoretical value of the  $FF$  increases by one simply coincide with the positions of the cusps in the critical field (b) Phase diagram for an open unique hole. Solid curve is the reduced critical field (or what is the same, the coherence length at  $T_{c3}^*$  normalised to the magnetic length). The same function for a blind hole with  $d_b/d_f = 0.382$  is shown by the dotted curve. Dashed lines show (for an open hole) the first order phase transition boundaries between states with different orbital momenta  $n$ .

From the above consideration it is clear that in general the filling factor is determined at the moment of the nucleation of superconductivity near a hole. At the same time there is some probability that the  $FF$  is increased by one during the field cooling. Therefore it is more convenient to consider the minimum possible (experimental) value of the filling factor  $FF_{\min}$  for holes of each radius. This value should be closer (than  $\langle FF \rangle$ ) to the number of vortices which nucleate inside each hole at  $T_{c3}^*$ . In Fig. 4a we compare the experimental data for  $FF_{\min}$  (solid circles) with the theoretical filling factor  $FF = n$  (solid line) which is determined from positions of the cusps in Fig. 4b and corresponds to  $T = T_{c3}^*$ . One can see a good agreement between the theory and experiment. The averaged experimental value of the filling factor  $\langle FF \rangle$  is somewhat higher than the  $FF$  calculated for  $T = T_{c3}^*$  but the difference is small (about one). It can be explained by first order

phase transitions in the interval  $T_{c2} < T < T_{c3}^*$ . For a more accurate quantitative treatment of this effect one should find exact positions of the first order phase transition boundaries by taking into account the screening effects and also by analysing possibilities of such transitions at  $T < T_{c2}(H)$ .

### 4.3. Stepwise Behaviour of the $\langle FF \rangle$

Our important experimental observation is the quantization of the *averaged* (over an array of holes) filling factor which reflects the fact that each hole capture the same number of vortices and this number is constant in some finite intervals of  $R$ . Such a “coherence” between remote holes is especially surprising if one takes into account that the experimental values of  $\langle FF \rangle$  are very different from their equilibrium values as it is shown above. The explanation naturally follows from the consideration of the edge superconducting states. Really we have seen (Fig. 2) that the interaction between the holes is negligible if  $a > 6 \mu\text{m}$ . Therefore the same number of vortices should be nucleated at  $T_{c3}^*$  in each hole. This number can not be influenced by such fluctuating from one hole to another factors as the intrinsic pinning in the Nb film or the relative position of the hole with respect to the Abrikosov lattice (just because there are no Abrikosov vortices at  $T_{c3}^*$ ). The subsequent cooling can cause the first order phase transition, but it increases the filling factor only by unity and should take place in all holes at the same time. Below  $T_{c2}$  a change in the filling factor is not probable because of the strong maximum of the order parameter near the hole edge at high temperatures and due to the intrinsic pinning at lower temperatures (see the above discussion). We come to the conclusion that the filling factor in the field cooling experiments should be determined only by the magnetic flux of the external field through the hole (in the agreement with the experimental result shown in Fig. 3), because this is the only parameter which determines the nucleation (and evolution in the GLL) of the edge superconducting states (Fig. 4b).

The role of the hole bottom in the nucleation process is analysed in details in<sup>(15)</sup> where it is shown that the critical field is very sensitive to the ratio  $d_b/d_f$  while the number of vortices which nucleate inside a hole decreases very weakly with the increasing bottom thickness. This fact is illustrated by the proximity of the two theoretical curves in Fig. 4a for open (solid line) and blind (dashed line) holes (see also Fig. 4b for comparison of the critical fields of blind and open holes).

## 5. TRANSITION INTO COLLECTIVE STATE

Till now we considered holes as independent objects but if the distance between them is comparable or smaller than  $\xi(T)$  then the interaction is

important and in the limit  $R \rightarrow a/2$  we come to the opposite case of a dense hole network which is similar to the wire network.<sup>13</sup> Let us discuss here the influence of such interhole interaction on the vortex distribution and on the transport properties just below the superconducting transition (in other words in the GLL).

### 5.1. Visualisation of Vortex Distribution

In the Fig. 2 (solid dots) one can see the dependence of  $\langle FF \rangle$  versus the hole radius obtained on hole arrays with the smallest lattice parameter  $a = 3.2 \mu\text{m}$ . When  $R$  is small enough, the data for  $a = 3.2 \mu\text{m}$  and for well separated holes with  $a = 6.1 \mu\text{m}$  or  $a = 12 \mu\text{m}$  coincide with each other. An increase of  $R$  leads to a more rapid growth of the  $\langle FF \rangle$  in the array with the highest density of holes. Finally at  $R_c \approx a/4$  the system comes to a new, “collective” state when the filling factor is saturated and equal to the frustration ( $FR$ ) of the lattice of holes:  $\langle FF \rangle = FR$ . The frustration is the averaged number of vortices per a unit cell:  $FR = \alpha a^2 H / \phi_0$ ,  $\alpha = 1$  for the square lattice and  $\alpha = \sqrt{3}/2$  for the triangular lattice. Note that the transition into the “collective” regime takes place when the distance between hole edges is approximately equal to the hole diameter  $2R$  i.e. when the edge superconducting states of neighbouring holes are considerably overlapped at the nucleation temperature,<sup>19</sup> but much earlier than the holes touch each other geometrically. The character of this transition is clear from Fig. 5 where we present images of two samples, one before and one after the saturation of  $\langle FF \rangle$ , decorated at the same time and at the same conditions. The only difference between them is the hole radius (the distance between the holes is the same). When the radius is small we find the “single-object” behaviour when almost each hole capture the same number of vortices (in Fig. 5a each hole capture two vortices while residual vortices are outside holes), and consequently the  $\langle FF \rangle$  in such state is an integer number determined by  $R$  and  $H$  in accordance with the phase diagram of a single hole.<sup>18</sup> The increase of  $R$  initiate the transition into the “collective” state when all vortices are captured (Fig. 5b), and the filling factor depends only on the relative positions of holes ( $\langle FF \rangle = \alpha a^2 H / \phi_0$ ) but not on their individual characteristics such as the radius.

### 5.2. First Order Transition

A simultaneous entrance of all free vortices inside holes at some critical value of the coherence length or at some critical hole radius is, by definition, a first order phase transition because it leads to a finite change of the state of the vortex crystal, but not only of its symmetry.<sup>20</sup>



Qualitatively speaking, the transition can be found from the comparison of the free energy of an additional probe vortex located inside a hole ( $F_0$ ) and in the middle between neighbouring holes forming a unit cell ( $F_1$ ). The condition for the “single-object” state is  $F_1 < F_0$ . Evidently it is fulfilled if the filling factor and the interhole separation are big enough, because the vortex energy in interstices is proportional to the order parameter amplitude and therefore decreases exponentially with the increasing  $a$ . At the same time the energy of a trapped vortex rises with the filling factor, if  $FF$  is sufficiently large. The transition into the “collective” state appears when  $F_1 = F_0$ . Experimentally we have found (Fig. 5b) that at sufficiently large  $R$  all vortices are trapped so the condition  $F_1 > F_0$  is fulfilled. It is in a qualitative agreement with the well known theoretical result that vortices do not exist in a film thinner than the coherence length<sup>21</sup> (if the field is parallel to the film). In our case the coherence length should be compared with the size of the superconducting region confined between neighbouring holes. The “superheating” line can be determined from the condition that the minimum of the energy in interstices ( $F_1$ ) becomes a maximum. It should be emphasised also that the first order transition corresponding to the entrance of an additional vortex inside a hole analysed in ref. 18 is a different phenomenon, because it corresponds to a single isolated hole and initiated by the decreasing temperature. Now we are discussing a collective phenomenon which takes place in a periodic lattice of holes. The transition from the “single-object” to the “collective” state takes place when the coherence length exceeds the separation between the holes, what leads to the expulsion of all vortices from the superconducting material to the holes. An increase (but not a decrease) of the temperature should lead to such redistribution.

### 5.3. Critical Temperature Oscillation

The above described transition helps to understand the results of our resistive measurements carried out on thin Al films with a square lattice of holes (all the experimental conditions are the same as in ref. 10). Firstly let us consider the critical temperature  $T_{c3}^*(H)$  of the perforated film.<sup>(10)</sup> In the derivative shown in Fig. 6b one can distinguish two types of oscillation. The large period found at high fields corresponds approximately to the increase of the magnetic flux through the hole area by one flux quantum. The structure at low fields is periodic peaks; the period exactly corresponds to one flux quantum through the area of a unit cell of the hole lattice. The sharp transition between these two types of the critical temperature oscillation can be completely explained if one takes into account that at the moment of superconductivity nucleation the system can be either in the

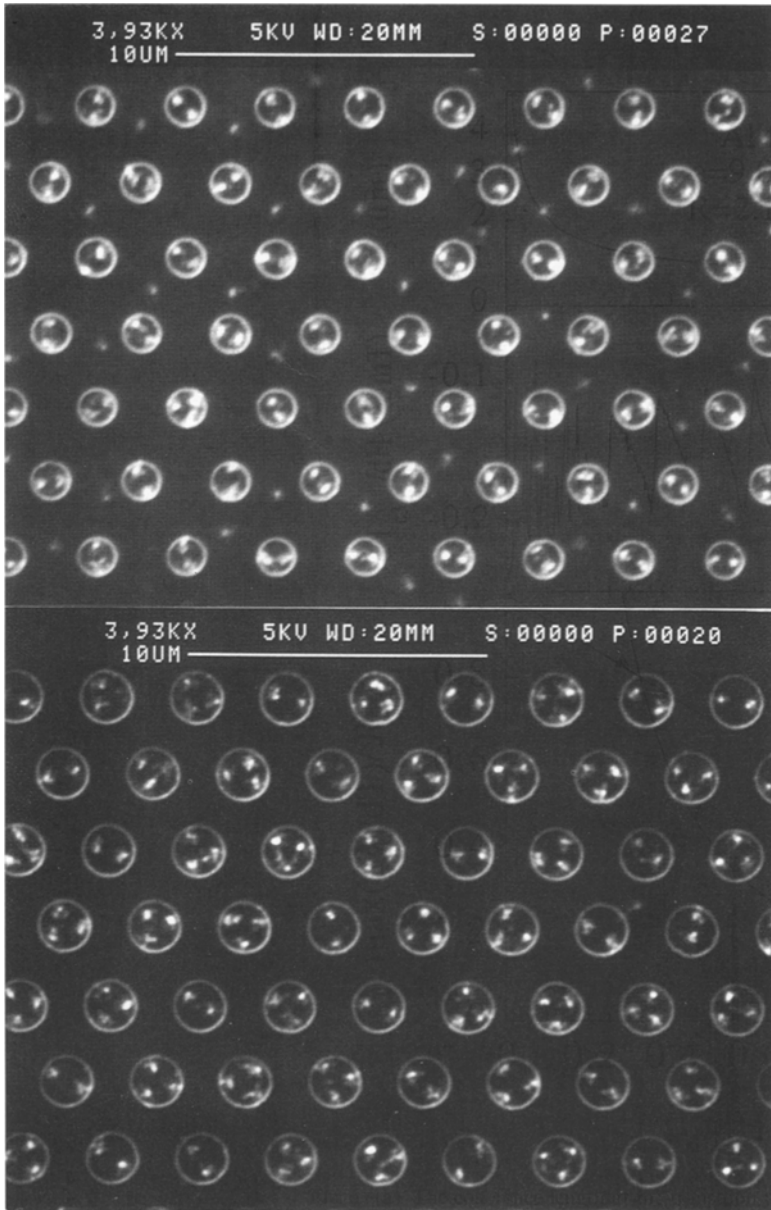


Fig. 5. Micrographs of two parts of the sample with arrays of holes of different radius ( $R=0.6\ \mu\text{m}$  and  $R=0.83\ \mu\text{m}$ ). The distance between holes in both cases is  $a=3.2\ \mu\text{m}$ . An increase of the hole radius leads to the transition from the “single-object” state (top picture, a) when the holes are independent and capture the same number of vortices into the “collective” state (bottom picture, b) when all vortices are inside holes and the averaged filling factor is equal to the frustration of the network of holes. The decoration is done after the cooling at  $H=6.37\ \text{Oe}$  down to  $T_{dec}=4.2\ \text{K}$ . The vortices are visible as white spots.

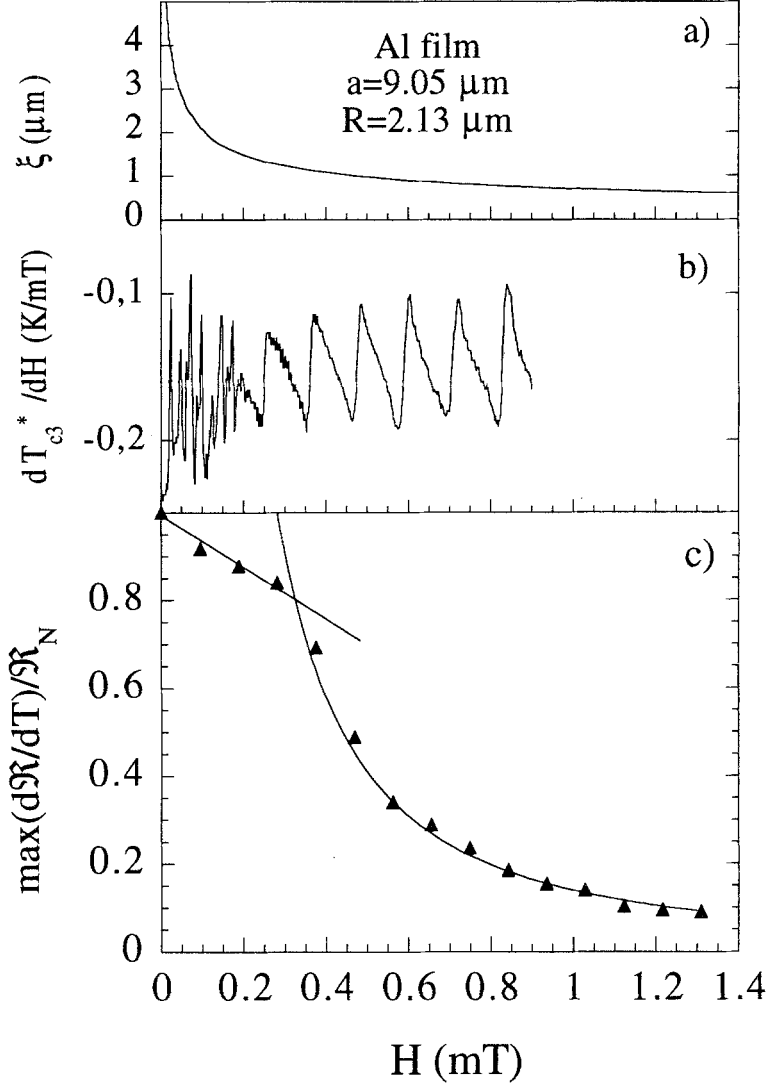


Fig. 6. (a) The coherence length at the transition temperature  $\xi[T_c^*(H)]$  in the Al perforated film used for the critical temperature and transport measurements (but not in the decoration experiments). It should be compared with the period of the hole lattice  $a=9.05 \mu\text{m}$  and the hole radius  $R=2.13 \mu\text{m}$ ; (b) The derivative of the critical temperature versus magnetic field for the same Al film. It shows the fast “collective” and the slow “single-object” oscillation; (c) The amplitude of the peak in the derivative of the Al film resistance versus the temperature (the experimental points are shown by triangulars). The horizontal axis is the external magnetic field, which is perpendicular to the film plane. Solid lines are the mean square fits.

“collective” or in the “single-object” state. The oscillation of  $T_{c3}^*$  with the large period corresponds to the “single-object” state when each hole capture the same number of vortices. A synchronized entrance of an additional vortex in each hole causes, similarly to the Little-Parks effect, a cusp in the critical temperature and a jump in the derivative. Naturally such transitions are repeated when the flux through the hole area is increased approximately by one flux quantum. At small fields the  $\xi[T_{c3}^*(H)]$  is sufficiently large in comparison to the interhole separation, what leads to the realisation of the “collective” state (the coherence length at the nucleation temperature is plotted in Fig. 6a). In this state, if  $H$  is arbitrary chosen, the  $FF$  is no more the same for different holes (as in Fig. 5b) since all vortices are inside holes and their total concentration is determined by the applied field. Now singularities in the critical temperature appear, as in wire networks, when  $FR$  is integer because in such case the  $FF$  is again the same for all holes. Therefore the period of the oscillation in the “collective” state is exactly equal to one flux quantum per the area of the unit cell of the hole lattice. Moreover if  $FR$  is a simple rational number, then the vortices are forming a commensurate superlattice.<sup>22</sup>

#### 5.4. Transport Properties (TAFF) near Superconducting Transition

An analysis of the thermally assisted flux flow (TAFF)<sup>23</sup> just below the superconducting transition gives another experimental evidence of the transition from the “collective” to the “single-object” state, which is governed again by the coherence length. Experiments are carried out on the same Al perforated film as in the pervious case and as in the ref. 10). They show that the magnetic field can cause not only the shift and the splitting of the resistive transition, but also its broadening (see Fig. 2 in the ref.10). This broadening is due to the thermally activated motion of vortices in the direction of the Lorentz force. It is linear with the driving current (when the current is small enough) so one can introduce the resistance of the sample ( $\mathfrak{R}$ ). From the general point of view, one can expect that the capturing of all vortices inside holes should lead to a qualitative change of the transport properties, in particular of the TAFF (which is considerable only near  $T_{c3}^*$ ). To characterise the broadening of the transition we use the derivative  $d\mathfrak{R}/dT$ . It has a peak when the superconductivity appears in the system; the amplitude of this peak is inversely proportional to the broadness of the transition and therefore should be a good characteristics of the TAFF. The result is shown in Fig. 6c, where we normalise this derivative by the sample resistance in the normal state ( $\mathfrak{R}_N$ ). One can see two different behaviours: at low fields when the coherence length at the superconducting transition  $\xi[T_{c3}^*(H)]$  is big, the “collective” state is realised. It implies the total capturing of vortices by holes, a weak

TAFF, and consequently a high peak in the derivative which decreases linearly with the field. Starting from some critical field, which in our particular case is  $H_{cs} \approx 0.3 \mu T$ , the height of the maximum decreases with the power law ( $\propto H^{-3/2}$ ). The simplest explanation of this change of the TAFF is to assume that at  $H = H_{cs}$  the system switches to the “single-object” state. This means that a part of vortices exits the holes, what gives rise a rapid increase of the TAFF (because the vortices between the holes are weakly bounded) and to the broadening of the transition. The disappearance of the “collective” oscillation (which is also explained by the delocalisation of vortices in the previous paragraph) takes place approximately at the same field  $\tilde{H}_{cs} \approx 0.2 mT$  (see Fig. 6b). The difference can be explained by the fast decay of the oscillation of the critical temperature, which is a usual phenomenon in the wire networks made of relatively thick wires.<sup>13, 24</sup> It should be mentioned that the result presented here is a preliminary one. Additional measurements of transport properties of perforated samples in the GLL should be of interest. For example one can expect to observe a reentrance effect. Namely the increase of the temperature leads to the increase of the coherence length and therefore to the transition into the “collective” state when all vortices enter the holes. Therefore the critical current of the perforated film should exhibit a jumpwise increase with increasing temperature. A re-entrant flux creep rate behaviour due to the multiquanta vortex formation was found recently in<sup>25</sup> in a perforated film, but probably this phenomenon is not related to the spatial modulation of the order parameter amplitude and should be discussed in the framework of the LL.

## 6. CONCLUSION

The Bitter decoration technique was used for the direct observation of the vortices trapped inside microholes. We have found that the number of fluxoids inside an isolated hole is determined by the edge superconducting state at  $T_{c3}^*$  and changes weakly during the field cooling due to the strong surface barrier and the intrinsic pinning. The density of fluxoids is much higher inside holes than outside and moreover the dependence of the averaged filling factor on the magnetic flux is stepwise. If the holes are close enough to each other so the separation between their edges is of the order of the coherence length, then the transition from the “single-object” to the “collective” state is possible. This transition is characterised by the sudden entrance of all vortices inside holes and corresponding saturation of the filling factor. It is found both in the decoration experiments and also by measuring the resistance of a perforated film when the above mentioned transition leads to a qualitative change of the TAFF process and of the critical temperature dependence on the magnetic field. The presence of a thin bottom in holes does not change the physics of vortex capturing but

provides a direct way to determine the number of trapped fluxoids (by the Bitter decoration). This method of the "flux compression" should be useful in the decoration of wire networks and others artificial mesoscopic systems. Our results show that the analysis of the vortex pinning near the second critical field by a system of empty channels or by the columnar defects is not possible without taking into account the surface superconducting states or in other words the strong nonuniformity of the order parameter.

We are very grateful to O. Buisson, A. Buzdin, A. Eichenberger, J. L. Genicon, B. Grebenschikov, A. Neminskii, and Yu. N. Ovchinnikov for many useful discussions, to M. Ferlet for help in the decoration, and to D. A. Lisachenko for the careful reading of the manuscript. The work is supported by the CEE "SUPNET" contract ERBCGRCT920068.

## REFERENCES

1. G. S. Mkrtchyan and V. V. Shmidt, *Soviet Phys. JETP* **34**, 195 (1972).
2. B. Khalfin and B. Ya. Shapiro, *Physica C* **202**, 393 (1992).
3. A. I. Buzdin, *Phys. Rev. B* **47**, 11416 (1993).
4. L. D. Cooley and A. M. Grishin, *Phys. Rev. Lett.* **74**, 2788 (1995).
5. A. T. Fiory, A. F. Hebard, and S. Somekh, *Appl. Phys. Lett.* **32**, 73 (1978).
6. M. Baert *et al.*, *Europhysics Letters* **29**, 157 (1995).
7. Yu. N. Ovchinnikov, *Sov. Phys. JETP* **52**, 923 (1980).
8. P. G. De Gennes, *Superconductivity of Metals and Alloys*, W. A. Benjamin, Inc., New York (1966).
9. Yu. N. Ovchinnikov, *Sov. Phys. JETP* **52**, 755 (1980).
10. A. Bezryadin and B. Pannetier, *J. of Low Temp. Phys.* **98**, 251 (1995).
11. D. Saint-James and P. G. de Gennes, *Phys. Lett.* **7**, 306 (1963).
12. H. J. Fink, *Phys. Rev. Lett.* **14**, 309 (1965).
13. B. Pannetier, J. Chaussy, and R. Rammal, *Phys. Rev. Lett.* **53**, 1845 (1984); B. Pannetier, in *Quantum Coherence in Mesoscopic Systems*, Plenum, New York, 1991.
14. K. Runge and B. Pannetier, *Europhys. Lett.* **24**, 737 (1993).
15. A. Bezryadin, Yu. N. Ovchinnikov, and B. Pannetier, to appear in *Phys. Rev. B*.
16. At very low fields ( $H < 10$  Oe) a considerable deviation (not shown) from the curves in Fig. 3 is found. It is probably related to the fact that at such low field the difference between  $T_{c3}^*(H)$  and  $T_{c2}(H)$  starts to be smaller than the superconducting transition width (about 1 mK).
17. K. Runge, Ph.D. Thesis, Joseph Fourier University, Grenoble (1993).
18. A. Bezryadin, A. Buzdin, and B. Pannetier, *Phys. Rev. B* **51**, 3718 (1995).
19. The coherence length at  $T = T_c^*$  if  $n \sim 1$  is approximately equal to the hole radius:  $\xi \sim R$ . See the phase diagram for a single hole in Ref. 18.
20. L. Landau and E. Lifshitz, *Statistical Physics* (Pergamon Press, London, 1979).
21. M. Tinkham, *Introduction to Superconductivity* (McGraw-Hill, New York, 1975), Chap. 4-10.2, p. 135.
22. A. Bezryadin, A. Buzdin, and B. Pannetier, to appear in proceedings "Macroscopic-Quantum Phenomena and Coherence in Superconducting Networks," 2-5 March 1995, Frascati, Italy.
23. M. Tinkham, *Introduction to Superconductivity* (McGraw-Hill, New York), Chap. 5-7.1, p. 175; P. M. Kes *et al.*, *Supercond. Sci. Technol.* **1**, 242 (1989).
24. S. P. Benz *et al.*, *Phys. Rev. B* **38**, 2869 (1988).
25. M. Baert *et al.*, *Phys. Rev. Lett.* **74**, 3269 (1995).